Understanding the Effects of Concentration on the Solvation Structure of Ca^{2+} in Aqueous Solution. II: Insights into Longer Range Order from Neutron Diffraction Isotope Substitution

Yaspal S. Badyal,*,§ Adrian C. Barnes,‡ Gabriel J. Cuello,† and John M. Simonson

Aqueous Chemistry and Geochemistry Group, Chemical Sciences Division, Oak Ridge National Laboratory, Oak Ridge, Tennessee 37831-6110, H.H. Wills Physical Laboratory, Bristol University, Royal Fort, Tyndall Avenue, Bristol BS8 1TL, United Kingdom, and Institut Laue-Langevin, 6, rue Jules Horowitz BP 156-38042 Grenoble Cedex 9, France

Received: August 5, 2004; In Final Form: September 23, 2004

Although the Ca^{2+} aqua-ion is of great importance to biology and a key component of natural groundwaters, many details of the solvation structure and its behavior have remained either unexplored or controversial. We report the findings of a new neutron diffraction study, building upon the results of an earlier, complementary investigation with EXAFS (Fulton, J. L.; Badyal, Y. S.; Simonson, J. M.; Heald, S. M. *J. Phys. Chem. A* **2003**, *107*, 4688−4696). The common goal of both studies was to develop a much clearer and more consistent picture of the effects of concentration on the Ca^{2+} solvation structure. In particular, we have tried to elucidate the microscopic basis of a thermodynamic anomaly reported for ambient aqueous solutions of $CaCl_2$ at concentrations greater than approximately 4.0 *m*. By measuring the neutron scattering from isotopically distinct ($^{nat}Ca/^{44}Ca$) pairs of $CaCl_2$ aqueous solutions at two concentrations (4.0 and 6.4 *m*) in both light and heavy water, the uniquely detailed Ca−H and Ca−X (X = O, Cl, or Ca) pair distribution functions, and the changes in them with concentration, were determined. This type of second-order isotope difference experiment has only been applied successfully before to two other aqua-ions, Ni^{2+} and Cr^{3+}. Our findings confirm the lack of substantial change in the nearest atomic neighbor Ca−O environment and the virtual absence of Ca^{2+}−Cl^- contact ion pairing even at high concentration, as first indicated by the preceding EXAFS investigation. Instead, the principal change with concentration appears to be the entry of significant numbers of Cl^- ions into the *second* hydration shell around Ca^{2+} and the resulting formation of Ca^{2+}−OH_2−Cl^- solvent-shared ion pairs. Our results provide compelling evidence for this picture, in particular the impact on the water hydrogen structure in the second hydration shell and the apparent effects on the tilt angle distribution of water molecules in the first hydration layer. The average number of water molecules in the first hydration shell of Ca^{2+} is close to 7 at both concentrations (although a small decrease with concentration is noticeable). Given the great rigor and consistency required for second-order isotope difference experiments, our values for coordination number and other structural parameters should be regarded as the benchmarks for this system. The pair distribution functions will also serve as an exacting test of theoretical and simulation models.

Introduction

A detailed knowledge of the solvation structure around electrolytes in aqueous solution is crucial to understanding the many chemical and biochemical processes that occur in the liquid phase. This is especially true of the Ca^{2+} ion, which plays key roles in a number of processes in advanced biological systems, for example, the triggering of muscle and nerve action.[1] Not surprisingly, the great importance of this aqua-ion to biology has prompted a number of studies of the hydration structure albeit at concentrations much greater than those found in living cells. Despite these efforts, a clear and consistent picture of Ca^{2+} hydration has yet to emerge, with widely differing results being reported for the average water coordination number and the nearest-neighbor Ca−O distance.[2] These problems can be ascribed, at least in part, to the weak and asymmetric nature of the Ca−O nearest-neighbor interaction.[3] The experimental difficulties are further compounded by such factors as the low atomic number of the element, which poses particular problems for structural methods based on the use of X-rays, and the ambiguities inherent in modeling total scattering data, where the solute−solvent correlations of interest often comprise only a small proportion of the measured scattering. The importance of this problem has spurred many theoretical investigations,[4−6] including several recent ab initio molecular dynamics studies.[7,8] However, the inconsistencies between experiment also find some parallel in the variable results of simulation. For example, Guàrdia et al.[4] report that structural parameters for the hydrated Ca^{2+} ion, in particular the first-shell coordination number, vary widely depending on the choice of ion−water potential adopted in their molecular dynamics simulations. The only other reported neutron diffraction isotope substitution (NDIS) experiment on $CaCl_2$ aqueous solutions (at generally lower concentrations than the present study) by Hewish et al.[9] makes the intriguing suggestion that the Ca^{2+} aqua-ion is weakly hydrated in the sense that the local structure is readily influenced by thermo-

* To whom correspondence should be addressed. E-mail: badyalys@ornl.gov. Fax: 865-241-4829.
§ Oak Ridge National Laboratory.
‡ Bristol University.
† Institut Laue-Langevin.

10.1021/jp046476c CCC: $27.50 © 2004 American Chemical Society
Published on Web 12/02/2004

dynamic factors such as concentration, type of counterion, and temperature.

The common purpose of the neutron diffraction study described in this paper and the preceding EXAFS investigation (described in detail in the previous paper,[10] henceforth referred to as part I) is to develop a more consistent and detailed understanding of the Ca^{2+} solvation structure in aqueous solution. In particular, we have sought insights into the microscopic basis of the apparent anomaly in thermodynamic behavior reported for high concentrations. Using the ion interaction approach to model osmotic coefficient data for ambient aqueous solutions of $CaCl_2$, and those of another simple salt, $MgCl_2$, Phutela and Pitzer[11] observed a striking difference in behavior above a concentration of about 4.5 *m* (*m*, mol/kg water). Phutela and Pitzer speculated that this anomaly was due to significant structural rearrangements in concentrated $CaCl_2$ solutions, most likely the formation of substantial numbers of $Ca^{2+}-Cl^-$ contact ion pairs. In the absence of much direct information on the local structure of the Ca^{2+} aqua-ion in concentrated solution, this would seem to be a reasonable explanation given that there is (in principle) little or no free water available once the salt concentration exceeds approximately 4 *m*.

The EXAFS results described in part I, however, serve to largely discount the ion-pairing hypothesis put forward by Phutela and Pitzer. The Ca K-edge spectrum for a 6 *m* calcium(II) chloride solution, when compared to a dilute reference solution of the perchlorate, gives no indication of the changes (in particular, phase shifts) that would accompany the presence of significant numbers of Cl^- ions as nearest atomic neighbors of Ca^{2+}. Comparison of the pre-edge and near-edge (XANES) regions of the EXAFS spectrum for 6 *m* $CaCl_2$ to those for reference compounds, such as the crystalline hydrates, confirms the essential picture of completely hydrated Ca^{2+} ions even at this high concentration. The mean water coordination number of approximately 7 and Ca−O nearest-neighbor distance of 2.44 Å are also broadly in agreement with earlier EXAFS studies on less concentrated solutions.[12] To summarize, the results described in part I present a consistent picture of the nearest-neighbor environment around Ca^{2+} in aqueous solution and reveal it to be largely unperturbed even at high concentration. The EXAFS study also confirms the relatively weak nature of the $Ca^{2+}-$water interaction as manifest by the low symmetry of the first coordination shell and the behavior in mixed solutions with $MgCl_2$.

Another powerful and selective means of probing the structure around ions in aqueous solution is of course provided by NDIS. The technique forms a strong complement to EXAFS in that it not only probes the nearest-neighbor region but also yields unique information on the longer-range structure. This is particularly important given the suggestion in part I that the principal change in concentrated $CaCl_2$ aqueous solutions is the formation of $Ca^{2+}-OH_2-Cl^-$ *solvent-shared* ion pairs rather than the contact ion pairs originally suggested by Phutela and Pitzer. In this paper, we report the findings of a neutron diffraction study on concentrated $CaCl_2$ aqueous solutions using calcium ($^{nat}Ca/^{44}Ca$) isotope substitution in both light and heavy water (i.e., also using H/D substitution). This method requires a high degree of care in experimentation and analysis to yield reliable second-order scattering differences, and has been applied successfully before to only two aqua-ions, Ni^{2+} and Cr^{3+}.[13,14] Two concentrations, nominally 6.4 and 4.0 *m* $CaCl_2$, were measured under ambient conditions with the D4c diffractometer of the Institut Laue-Langevin, Grenoble. Combining the unique information on longer range structure provided by the present NDIS study with the insights into local atomic structure supplied by EXAFS in part I allows us to form the clearest picture to date of the effects of concentration on the Ca^{2+} solvation structure.

TABLE 1: Cross Sections and Coherent Scattering Lengths Used in Data Analysis[a]

		cross sections (barns, 10^{-28} m^2)	
	$\bar{b}$ (10^{-14} m)	σ_{coh}	σ_{incoh}
^{nat}Ca	0.476	2.847	0.043
^{44}Ca	0.18	0.4072	0.0028
Cl	0.9577	11.53	5.3
O	0.5803	4.232	0.0008
D	0.6671	5.592	2.05
H	−0.374	1.757	80.26

[a] The values are from Sears.[15] The total scattering cross section is given by $\sigma_{scat} = \sigma_{coh} + \sigma_{incoh.}$

Experimental Methods and Theory

Sample Preparation. Isotopic ^{44}Ca (98.89% enrichment) was obtained in the form of the carbonate from the isotope production and distribution facility at Oak Ridge National Laboratory. This was converted into the chloride by reaction with concentrated hydrochloric acid. Since the carbonate is practically insoluble, it could be titrated with drops of acid until no solid remained visible, leaving behind only a dissolved solution of the chloride. Any small amounts of excess acid (pH readings never deviated far from neutral) were removed by heating these intermediate solutions to dryness before adding appropriate amounts of light or heavy water to make up the final, concentrated (∼6.4 *m*) sample solutions. To limit contamination with hydrogen, deuterated acid (37 wt %, 99 atom % D, Aldrich) was used to convert the carbonate for the ^{44}-$CaCl_2$ heavy water sample. In principle, the heavy water solution containing natural enrichment calcium(II) chloride should also have been prepared in the same way (so as to minimize differences in deuterium enrichment). In practice, difficulties were encountered with the purity of the carbonate starting material so the natural solution samples were finally made directly by using ultra-dry $CaCl_2$ (<100 ppm of H_2O, Johnson Matthey) and enriched D_2O (99.9 atom % D, Aldrich) or nanopure H_2O. Because of the difference in preparation methods, with the more rapidly prepared natural sample having less exposure to H_2O contamination, the heavy water solutions would inevitably differ somewhat in their deuterium enrichment. Given the very large incoherent scattering cross-section of hydrogen (see Table 1), such a H:D imbalance can have an appreciable affect on the measured isotope difference.[16] The details of how this anticipated problem was addressed during the actual neutron scattering experiment are given below in the section on fine-tuning experiment and analysis.

Neutron Scattering Methods. The neutron measurements were performed under ambient conditions with the D4c diffractometer instrument of the Institut Laue-Langevin (ILL), Grenoble.[17] The solutions were contained in a cylindrical, thin-walled $Ti_{68}Zr_{32}$ "null alloy" cell (9.5 mm o.d., 8.0 mm i.d.) mounted in an evacuated sample chamber. The rectangular beam incident on the sample was set at 10 mm wide and 35 mm high, and the nominal wavelength was fixed at 0.71 Å. Two pairs of isotopic and natural-enrichment Ca solutions, in light and heavy water, respectively, were each measured at two concentrations. To make the best use of the limited amount of ^{44}Ca isotope, the samples were initially prepared as the more concentrated

(nominally 6.4 *m*) solutions. Once these were measured, they were diluted to the lower concentration (nominally 4.0 *m*) and measured again. In addition to the samples, measurements also were made of the scattering from the empty cell, instrument, and cadmium rod backgrounds, as well as nickel powder and vanadium rod standards. Software available online at the D4c facility was used to correct for counter deadtimes, to normalize for detector efficiencies and the integrated flux on each sample, and to group data from different detectors. The known positions of Bragg peaks in the scattering from nickel powder were used to calibrate the measurements as a function of scattering angle 2θ before mapping to the scattering vector Q. Further analyses of the scattering data, including corrections for attenuation and multiple scattering, and subtraction of empty cell and other backgrounds, were carried out with standard programs.[18] Table 1 shows the scattering lengths and cross sections used in analyzing the data.

The Method of Isotope Scattering Differences. The NDIS method is already well documented[19] so a basic outline of the most relevant points will suffice here. The neutron scattering from a multicomponent liquid or amorphous sample is usually described in terms of the total structure factor, $F(Q)$, which in the Faber−Ziman formalism is given by

$$F(Q) = \sum_{\alpha,\beta} c_\alpha c_\beta \bar{b}_\alpha \bar{b}_\beta [S_{\alpha\beta}(Q) - 1] \quad (1)$$

where Q is the scalar form of the scattering vector ($Q = 4\pi \sin\theta/\lambda$, with 2θ being the scattering angle and λ the wavelength of the incident neutrons). In the above expression, c_α is the concentration and $\bar{b}_\alpha$ is the coherent scattering length of atomic species α. The static partial structure factor $S_{\alpha\beta}(Q)$ describes the correlations involving a given pair of atom types α and β. The total structure factor is simply the sum, weighted for concentration and neutron scattering length, over all partial structure factors pertaining to the sample. For a binary salt of the form MX_n (M is the metal, X is the halide, n is the valence of M) in aqueous solution, $F(Q)$ contains 10 distinct terms and for a solution in D_2O can be explicitly written as

$$\begin{aligned} F(Q) = {} & K_{O-O}[S_{O-O}(Q) - 1] + K_{O-D}[S_{O-D}(Q) - 1] + \\ & K_{D-D}[S_{D-D}(Q) - 1] + K_{M-O}[S_{M-O}(Q) - 1] + \\ & K_{M-D}[S_{M-D}(Q) - 1] + K_{M-X}[S_{M-X}(Q) - 1] + \\ & K_{M-M}[S_{M-M}(Q) - 1] + K_{X-O}[S_{X-O}(Q) - 1] + \\ & K_{X-D}[S_{X-D}(Q) - 1] + K_{X-X}[S_{X-X}(Q) - 1] \quad (2) \end{aligned}$$

where the weighting coefficients $K_{\alpha\beta}$ ($=2c_\alpha c_\beta \bar{b}_\alpha \bar{b}_\beta$ for $\alpha \neq \beta$, treating $S_{\alpha\beta}(Q)$ and $S_{\beta\alpha}(Q)$ as equivalent, and $=(c_\alpha \bar{b}_\alpha)^2$ for $\alpha = \beta$) are in units of barns per steradian (1 barn $= 10^{-28}$ m^2). Fourier transformation of $F(Q)$ gives the average real-space pair distribution function, $G(r)$, which is weighted in the same way and has the analogous form

$$\begin{aligned} G(r) = {} & K_{O-O}[g_{O-O}(r) - 1] + K_{O-D}[g_{O-D}(r) - 1] + \\ & K_{D-D}[g_{D-D}(r) - 1] + K_{M-O}[g_{M-O}(r) - 1] + \\ & K_{M-D}[g_{M-D}(r) - 1] + K_{M-X}[g_{M-X}(r) - 1] + \\ & K_{M-M}[g_{M-M}(r) - 1] + K_{X-O}[g_{X-O}(r) - 1] + \\ & K_{X-D}[g_{X-D}(r) - 1] + K_{X-X}[g_{X-X}(r) - 1] \quad (3) \end{aligned}$$

where $g_{\alpha\beta}(r)$ are the partial pair distributions as functions of the radial distance between pairs of atoms, r. In the above equation, the first three terms (O−O, O−D, and D−D) are associated with the solvent structure and dominate the total scattering whereas the remaining terms due to ion−water and ion−ion correlations are less strongly weighted. Isotopic substitution of the ion changes the scattering length and hence weighting coefficients of just the four terms involving that ion. Thus, in the present case of substituting the calcium ion, the first-order *difference* in scattering from a pair of matched D_2O solutions reduces to

$$\begin{aligned} \Delta G^{D}_{Ca}(r) = {} & \Delta K_{Ca-O}[g_{Ca-O}(r) - 1] + \Delta K_{Ca-D}[g_{Ca-D}(r) - \\ & 1] + \Delta K_{Ca-Cl}[g_{Ca-Cl}(r) - 1] + \Delta K_{Ca-Ca}[g_{Ca-Ca}(r) - 1] \quad (4) \end{aligned}$$

where $\Delta K_{Ca-O} = 2c_{Ca}c_O(\bar{b}^{nat}_{Ca} - \bar{b}^{44}_{Ca})\bar{b}_O$, $\Delta K_{Ca-D} = 2c_{Ca}c_D(\bar{b}^{nat}_{Ca} - \bar{b}^{44}_{Ca})\bar{b}_D$, $\Delta K_{Ca-Cl} = 2c_{Ca}c_{Cl}(\bar{b}^{nat}_{Ca} - \bar{b}^{44}_{Ca})\bar{b}_{Cl}$, $\Delta K_{Ca-Ca} = c_{Ca}{}^2((\bar{b}^{nat}_{Ca})^2 - (\bar{b}^{44}_{Ca})^2)$. Because there is more solvent than solute ($c_D = 2c_O \gg 2c_{Ca} = c_{Cl}$), the first two ion−water terms are the most significant even at high salt concentration. The NDIS method thus provides selective information on the *hydration* structure around the substituted ion. At radial distances r shorter than the closest approach of atoms, all $g_{\alpha\beta}(r)$ go to zero and the difference reduces to a constant given by

$$\Delta G^{D}_{Ca}(0) = -(\Delta K_{Ca-O} + \Delta K_{Ca-D} + \Delta K_{Ca-Cl} + \Delta K_{Ca-Ca}) \quad (5)$$

providing a useful check on the normalization of the data and the effectiveness of data correction procedures.

Since the bulk scattering from the solvent cancels out in a first-order isotope difference, the same calcium isotope substitution can also be carried out in H_2O to yield

$$\begin{aligned} \Delta G^{H}_{Ca}(r) = {} & \Delta K_{Ca-O}[g_{Ca-O}(r) - 1] + \Delta K_{Ca-H}[g_{Ca-H}(r) - \\ & 1] + \Delta K_{Ca-Cl}[g_{Ca-Cl}(r) - 1] + \Delta K_{Ca-Ca}[g_{Ca-Ca}(r) - 1] \quad (6) \end{aligned}$$

which only differs from eq 4 in that $\Delta K_{Ca-H} = 2c_{Ca}c_H(\bar{b}^{nat}_{Ca} - \bar{b}^{44}_{Ca})\bar{b}_H \neq \Delta K_{Ca-D}$ because the H and D coherent scattering lengths are different. Assuming H and D can be treated as isomorphic (i.e., $g_{Ca-D}(r) = g_{Ca-H}(r)$), it is straightforward to show that the two first-order differences (eqs 4 and 6) can be combined to give the following second-order differences

$$g_{Ca-H}(r) = 1 + \frac{\Delta G^{D}_{Ca}(r) - \Delta G^{H}_{Ca}(r)}{\Delta K_{Ca-D} - \Delta K_{Ca-H}} \quad (7)$$

and

$$g_{Ca-O}(r) + \chi(r) = 1 + \frac{k\Delta G^{D}_{Ca}(r) + \Delta G^{H}_{Ca}(r)}{\Delta K_{Ca-O}(k+1)} \quad (8)$$

where $k = |\bar{b}_H/\bar{b}_D|$. Note that $g_{Ca-H}(r)$ is obtained from eq 7 exactly, but the expression for $g_{Ca-O}(r)$ contains an error term, $\chi(r)$, from Ca−Cl and Ca−Ca correlations, which can be explicitly written as

$$\chi(r) = \frac{\Delta K_{Ca-Cl}[g_{Ca-Cl}(r) - 1] + \Delta K_{Ca-Ca}[g_{Ca-Ca}(r) - 1]}{\Delta K_{Ca-O}} \quad (9)$$

Although $\Delta K_{Ca-O} > \Delta K_{Ca-Cl}$ and $\Delta K_{Ca-O} \gg \Delta K_{Ca-Ca}$, $\chi(r)$ is too large at the high concentrations of the present study to be neglected. In addition to information on peak shapes and positions, pair distribution functions also yield coordination numbers according to the formula

$$\bar{n}^{\beta}_{\alpha} = \rho c_\beta \int_{r1}^{r2} 4\pi r^2 g_{\alpha\beta}(r)\, dr \quad (10)$$

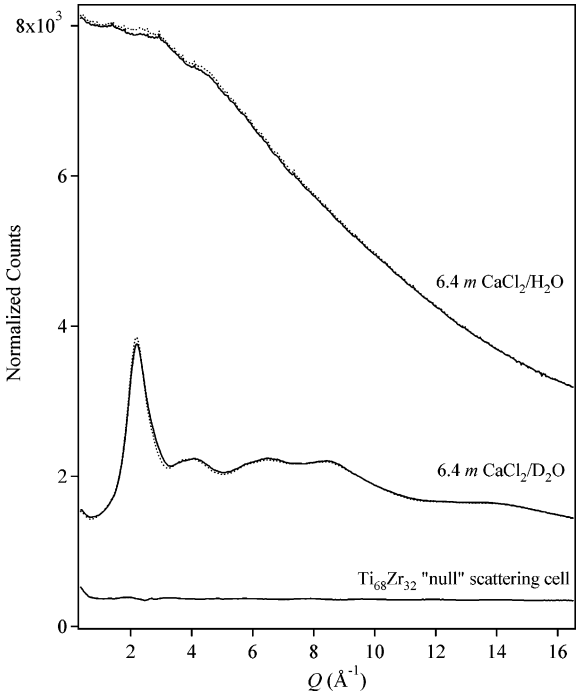

Figure 1. Comparison of the total scattering from pairs of concentrated (nominally 6.4 *m* $CaCl_2$) light and heavy water solutions containing ^{nat}Ca (solid curves) and isotopic ^{44}Ca (dotted curves). The data are uncorrected except for counter deadtime and are normalized to the same number of monitor counts. A large and distinctive contribution from hydrogen incoherent scattering is evident in the light water samples, the effects of inelasticity giving rise to a sharp fall off with increasing *Q*.

where $\bar{n}_\alpha^\beta$ is the average number of β atoms around a central atom of type α, ρ is the total number density (atoms/Å^3), and integration is over a spherical shell of inner radius $r1$ and outer radius $r2$.

Fine-Tuning Experiment and Analysis. Because isotope scattering differences are small ($\sim$1−2%) compared to the measured total scattering, the success of the isotope substitution method clearly depends on the samples being otherwise very similar. Systematic errors from poorly matched samples can have a significant effect on the desired isotope difference. Before discussing our findings in detail, we describe the steps taken, both during and after experiment, to identify and minimize the impact of such errors thereby ensuring the validity of the final results.

Figure 1 compares the total scattering for pairs of concentrated $CaCl_2$ solutions in light and heavy water. The data are uncorrected except for counter deadtime and the time-integrated flux on sample. The large incoherent scattering of hydrogen, with its characteristic rapid falloff with increasing *Q* due to inelasticity effects, is clearly evident from the light water data. This characteristic signature can be used to check the relative levels of hydrogen contamination in the *heavy water* solutions. Figure 2 shows the initial first-order difference of the raw scattering data and, as anticipated, there were clear signs of a difference in deuterium enrichment, with the ^{44}Ca solution in D_2O containing slightly more hydrogen than the ^{nat}Ca sample. Before continuing with the experiment proper, the imbalance in deuterium enrichment was corrected by progressively titrating the "better" ^{nat}Ca heavy water solution with drops of H_2O. After each drop was added, the sample scattering was remeasured and the first-order scattering difference recalculated until it was evident that the H:D imbalance had largely been corrected (upper curve in Figure 2). The deuterium enrichment of the ^{nat}Ca sample had to be shifted by about 1% H to achieve the desired result. No further adjustments were made during the experiment except for diluting the samples so they could be measured at the lower concentration.

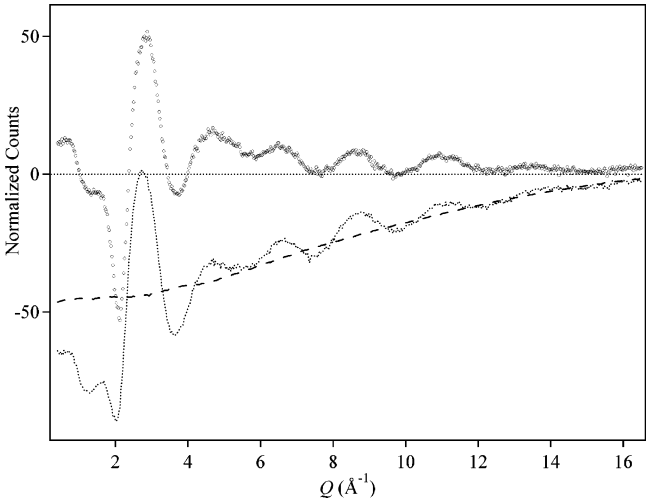

Figure 2. Comparison of the raw first-order scattering differences for the nominally 6.4 *m* $CaCl_2$ solutions in heavy water before (dotted curve) and after (open circles) titrating the ^{nat}Ca solution with H_2O. The slope evident in the uncorrected difference is clearly due to the subtraction of incoherent scattering from excess hydrogen in the ^{44}Ca sample. The shape of the apparent slope compares well with an estimate (long dashed curve) based on the total scattering of a light water sample (see Figure 1). Titration has largely corrected the imbalance in deuterium enrichment between the solutions.

Because striving to limit H_2O contamination tends to complicate the sample preparation process, isotope difference measurements with heavy water solutions may also be prone to other systematic errors such as mismatches in concentration. This point is illustrated in Figure 3, which shows the direct first-order difference (dotted curve) in real space, $\Delta G_{Ca}^{D}(r)$, for the concentrated solutions after completion of the formal data analysis process. The peak at $r \approx 0.95$ Å is readily identifiable as the O−D bond distance of molecular water and its presence indicates that the solvent contributions do not cancel out completely. Since any significant H:D imbalance had already been corrected during measurement, this remaining discrepancy can only be due to a small difference in concentration. As will become apparent later, no significant imbalances in concentration were indicated by the first-order differences for the *light water* samples. Checks of sample concentration with Raman, NMR, and atomic absorption spectroscopies led to the final values shown in Table 2, which are also closely consistent with indications from data analysis. The small, but appreciable, difference in concentration for the heavy water samples (6.31 *m* $^{nat}CaCl_2$ versus 6.25 *m* $^{44}CaCl_2$) introduces error terms related to the solvent scattering in the direct first-order difference as quantified in Table 3. (Note that for ease of comparison the values of the weighting coefficients $K_{\alpha\beta}$ have been multiplied by 10^3 and so are consistently tabulated in units of mbarns per steradian whereas the plotted data use the conventional barns per steradian.) An effective data analysis correction can be applied by slightly rescaling the total scattering from the ^{nat}Ca sample prior to subtracting the ^{44}Ca scattering. In this way, it is possible to compensate for the slightly lower solvent scattering in the more concentrated ^{nat}Ca solution and eliminate the O−D contribution in the first-order difference (solid curve in Figure 3). The weighting coefficients of the resulting corrected difference are also compared to those of the direct difference in Table 3. In addition to eliminating the O−D term, the improvements

TABLE 2: Sample Compositions for All Pairs of Solutions Studied[a]

solution	molality, *m*	density (atoms/Å^3)	atomic concentration					
			^{nat}Ca	^{44}Ca	Cl	O	H	D
$^{nat}CaCl_2/D_2O$	6.31	0.092	0.03403	–	0.06806	0.2993	0.007	0.5914
$^{44}CaCl_2/D_2O$	6.25		–	0.03374	0.06747	0.2996	0.006	0.5932
$^{nat}CaCl_2/H_2O$	6.49	0.092	0.0349	–	0.06981	0.2984	0.5969	–
$^{44}CaCl_2/H_2O$	6.475		–	0.03483	0.06967	0.2985	0.597	–
$^{nat}CaCl_2/D_2O$	4.0	0.096	0.02241	–	0.04482	0.3109	0.0075	0.6144
$^{44}CaCl_2/D_2O$	3.94		–	0.0221	0.04419	0.3112	0.0062	0.6163
$^{nat}CaCl_2/H_2O$	4.0	0.096	0.02241	–	0.04482	0.3109	0.6218	–
$^{44}CaCl_2/H_2O$	4.0		–	0.02241	0.04482	0.3109	0.6218	–

[a] Molality has been calculated consistently on the basis of moles of Ca per 55.5 mol of D_2O or H_2O (i.e., for the same number of moles of H_2O present in 1 kg of that solvent).

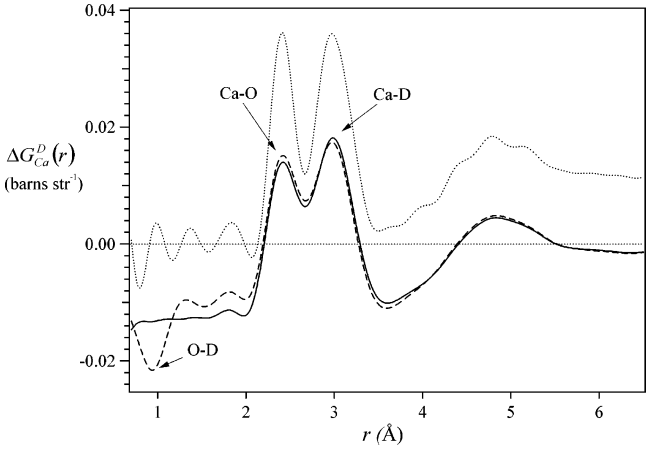

Figure 3. Real-space, first-order difference data for measurements in D_2O and at high concentration (nominally 6.4 *m* $CaCl_2$). Concentrating first on the two lower curves, the direct difference (dashed curve) indicates a small mismatch in concentration between the two solutions as evidenced by the intramolecular O−D peak of water at $r \approx 0.95$ Å. The imbalance in the solvent O−D and D−D contributions has been approximately corrected by applying a small rescaling factor (×1.012) to the scattering from the more concentrated ^{nat}Ca sample. The result is a clearly improved difference (solid curve) with good agreement in the water coordination numbers estimated from the individual peaks (labeled Ca−O and Ca−D) in the first hydration shell thus confirming the validity of the correction. The upper (dotted) curve, which has been displaced vertically by +0.013, shows the result of *not* applying a Lorch window function during Fourier transformation. In addition to the desired effect of minimizing termination ripple, the use of a window function clearly also results in significant broadening of the first hydration peaks (particularly Ca−O). This fact should be borne in mind when evaluating the real-space data presented in this paper (generated consistently by using a Lorch window and a Q_{max} cutoff of 16.5 Å^{-1}).

include a sharp reduction in the D−D contribution. Of the remaining error terms, the largest is due to D−Cl but even this only has a small weighting comparable to the most minor term (Ca−Ca) in the nominal isotope difference. In both cases, the normalization constant, $\Delta G^D_{Ca}(0)$, is consistent with the low-*r* region of the corresponding data in Figure 3. The validity of the much improved $\Delta G^D_{Ca}(r)$ that results from this correction is confirmed by the good agreement in the water coordination numbers (6.7 and 7.0, respectively) estimated from the individual Ca−O and Ca−D peaks in the first hydration shell. As shown later in the discussion, the highly consistent second-order differences that result from combining the first-order differences in light and heavy water provide even stronger confirmation that the data have been treated correctly.

Results and Discussion

The fully corrected, first-order scattering differences in heavy water, $\Delta F^D_{Ca}(Q)$, are compared for both concentrations in

TABLE 3: Values of Weighting Coefficients in the Direct and Corrected $\Delta G^D_{Ca}(r)$ for Concentrated $CaCl_2$ As Shown in Figure 3[a]

pair correlation α−β	$\Delta K_{\alpha-\beta} \times 10^3$ (mbarns str^{-1})	
	direct difference	corrected
Ca−O	3.480	3.510
Ca−D	7.836	7.903
Ca−Cl	1.314	1.325
Ca−Ca	0.224	0.226
O−D	−0.701	–
D−D	−1.282	−0.483
O−O	−0.059	0.098
Cl−D	0.233	0.292
Cl−O	0.175	0.292
Cl−Cl	0.074	0.096
$\Delta G^D_{Ca}(0) \times 10^3$	−11.29	−13.25

[a] The negative sum of the terms in each column gives the expected low-*r* constant value (last row). Correcting the difference eliminates the error term from O−D and sharply reduces the contribution from D−D. This improvement is at the expense of slight increases in the error terms from O−O and those correlations involving Cl. Fortunately, these unwanted contributions remain small compared to the desired terms involving Ca.

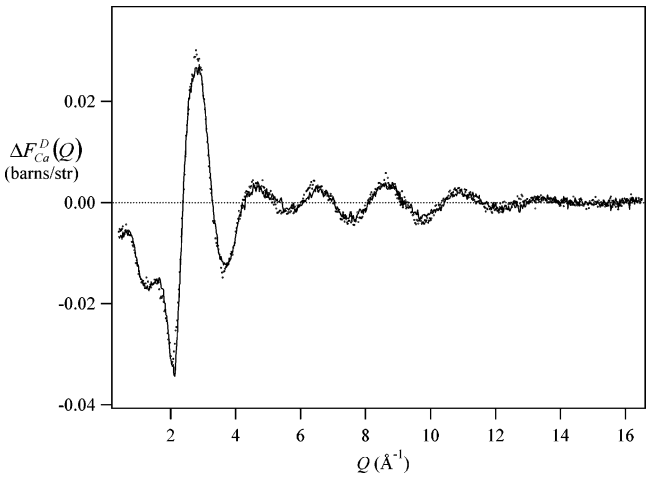

Figure 4. The first-order scattering differences in D_2O for both concentrations after all corrections have been applied. Residual slopes in the scattering data have been removed by correcting the low-*r* region below 0.8 Å in the corresponding $\Delta G^D_{Ca}(r)$ and back transforming. To allow direct comparison with the higher concentration data (solid curve), the data for 4.0 *m* $CaCl_2$ (dotted) have been scaled by the ratio of the Ca−O weightings (×1.45).

Figure 4. The basic features—a primary peak at $Q \approx 3$ Å^{-1}, preceded by a sharp dip at $Q \approx 2$ Å^{-1}, and followed by several smaller oscillations at higher *Q*—mirror those of other studies of well-hydrated ions, for example, Ni^{2+} in aqueous solution.[20]

TABLE 4: Weighting Coefficients for All First-Order Differences $\Delta G^{D}_{Ca}(r)$ and $\Delta G^{H}_{Ca}(r)$

	$\Delta K_{\alpha-\beta} \times 10^3$ (mbarns str^{-1})			
	6.4 *m* $CaCl_2$		4.0 *m* $CaCl_2$	
$\alpha-\beta$	$\Delta G^{D}_{Ca}(r)$	$\Delta G^{H}_{Ca}(r)$	$\Delta G^{D}_{Ca}(r)$	$\Delta G^{H}_{Ca}(r)$
Ca−O	3.510	3.540	2.409	2.370
Ca−H	7.903	−4.56	5.424	−3.054
Ca−Cl	1.325	1.368	0.578	0.564
Ca−Ca	0.226	0.235	0.098	0.097
O−H	−	0.036	−	−
H−H	−0.483	−0.024	−0.531	−
O−O	0.098	0.013	0.103	−
Cl−H	0.292	−0.053	0.527	−
Cl−O	0.292	0.041	0.282	−
Cl−Cl	0.096	0.018	0.061	−
$\Delta G^{D}_{Ca}(0) \times 10^3$	−13.25	−0.613	−8.95	0.023

[a] Note that a general reference to H means either H or D. The coefficients for the heavy water differences include the small correction for concentration imbalances as described in the main text.

To facilitate comparison, $\Delta F^{D}_{Ca}(Q)$ for 4.0 *m* $CaCl_2$ has been scaled up by the ratio of the Ca−O weighting coefficients (×1.45, see Table 4 where the weighting coefficients for all the first-order differences are tabulated). The changes with concentration appear rather subtle, mainly involving slight alterations in the shape and phase of the small peak at $Q \approx 6.5$ Å^{-1}. There is also some reduction in the amplitude of the main peak. This preliminary examination of the data suggests that the hydration structure of Ca^{2+}, while becoming slightly weaker at higher concentration, undergoes a perturbation rather than a substantial modification.

The real-space equivalents of the first-order scattering differences for both light and heavy water solutions are shown in Figure 5 (note that a Q_{max} cutoff of 16.5 Å^{-1} and a Lorch window were consistently used to Fourier transform the data). As indicated by the initial comparison of scattering differences, the Ca^{2+} hydration structure does not change dramatically with concentration. The most distinct change is the shift in position of the Ca−H peak in the first hydration shell, which starts off at $r = 3.03$ Å at low concentration and shifts down to $r = 2.98$ Å at the high concentration. This peak shift is seen consistently in both the light and heavy water differences. The Ca−H first peak distance at high concentration agrees closely with the value (2.97 Å) obtained in part I with use of EXAFS, although this earlier study was unable to detect the clear shift in this distance with concentration. Also consistent with our preceding study I, the Ca−O first peak distance does not change significantly with concentration although the absolute value is somewhat lower at 2.41 Å (compared to 2.44 Å from EXAFS). There is, however, a small discrepancy in the position of this peak in $\Delta G^{H}_{Ca}(r)$ as compared to $\Delta G^{D}_{Ca}(r)$ for 4.0 *m* $CaCl_2$, the origin of which is unknown. The subtle changes with increasing concentration are not limited solely to the first hydration shell—modifications in longer range order are also apparent. This is most easily seen by comparing the light water differences in Figure 5, for example, there is a peak at $r \approx 4.6$ Å at low concentration that moves out to $r \approx 4.7$ Å at high concentration. Because the Ca−H contribution is negatively weighted, whereas Ca−O is not, the orientational ordering of water molecules is more easily deduced from $\Delta G^{H}_{Ca}(r)$. In the case of 4.0 *m* $CaCl_2$, the positive peak at $r \approx 4.6$ Å is followed by a negative dip at $r \approx 5.6$ Å, which indicates that the second-shell water molecules are aligned in a similar way to those in the first hydration shell, i.e., with the negatively charged water oxygens closer to, and

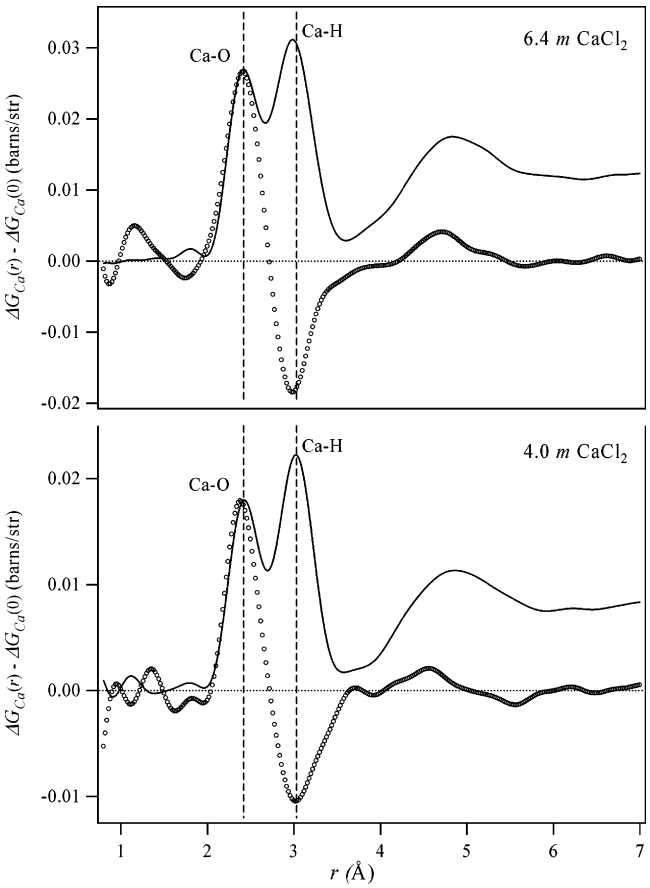

Figure 5. The collated real-space first-order difference data for both concentrations in D_2O (solid curves) and in H_2O (open circles). At low concentration, the Ca−O and Ca−D first peak positions are at $r \approx 2.41$ and 3.03 Å, respectively. The dashed vertical lines serve to highlight any changes in these peak positions at the higher concentration—most notably, the shift to lower r in the Ca−H peak distance. Note the lack of any obvious feature at $r \approx 0.95$ Å in the light water results, implying the solutions were closely matched in concentration.

the positively charged hydrogens further out and generally pointing away from, the central Ca^{2+} ion. At the higher concentration the negative contribution from Ca−H is less distinct, implying a weakening of the radial alignment of water molecules in the second hydration shell.

Having compared and established the consistency of the first-order differences, they can now be combined to form the more detailed and less ambiguous second-order differences. Results for the high concentration are plotted in Figure 6 and correspond to the following expressions

$$G_{Ca-H}(r) = [\Delta G^{D}_{Ca}(r) - \Delta G^{D}_{Ca}(0)] - 0.992[\Delta G^{H}_{Ca}(r) - \Delta G^{H}_{Ca}(0)] = 12.4 g_{Ca-H}(r) + E \quad (11)$$

$$G_{Ca-X}(r) = 0.57[\Delta G^{D}_{Ca}(r) - \Delta G^{D}_{Ca}(0)] + [\Delta G^{H}_{Ca}(r) - \Delta G^{H}_{Ca}(0)] = 5.5 g_{Ca-O}(r) + 2.1 g_{Ca-Cl}(r) + 0.36 g_{Ca-Ca}(r) + E' \quad (12)$$

in units of mbarns str^{-1}, where $E \cong -0.46 g_{H-H}(r) + 0.34 g_{H-Cl}(r) + 0.25 g_{O-Cl}(r)$ and $E' \cong -0.3 g_{H-H}(r) + 0.21 g_{O-Cl}(r) + 0.11 g_{H-Cl}(r)$ represent the most significant error terms. The conditioning of the second-order differences is excellent, with the Ca−O and Ca−H peaks in the first hydration shell appearing cleanly resolved. The high quality of the results is evidenced by the remarkably good agreement (to within 2%) in the water

TABLE 5: Parameters for the Ca^{2+} First Hydration Peaks As Derived from the Second-Order Differences $g_{Ca-H}(r)$ and $g_{Ca-O}(r) + \chi(r)$[a]

	r_{Ca-O} (Å)	Δr_{Ca-O} (Å)	$\bar{n}^{O}_{Ca}$	r_{Ca-H} (Å)	Δr_{Ca-H} (Å)	$0.5\,\bar{n}^{H}_{Ca}$
6.4 *m* $CaCl_2$	2.41(0.01)	0.32(0.02)	6.95(0.1)	2.98(0.01)	0.46(0.02)	6.84(0.1)
4.0 *m* $CaCl_2$	2.40(0.01)	0.31(0.02)	7.3(0.1)	3.03(0.01)	0.46(0.02)	7.25(0.1)

[a] The peak positions, r_{Ca-O} and r_{Ca-H}, full-widths at half-maximum, Δr_{Ca-O} and Δr_{Ca-H}, and average water coordination numbers calculated independently from the Ca−O and Ca−H first peaks, $\bar{n}^{O}_{Ca}$ and $0.5\bar{n}^{H}_{Ca}$, are presented. The estimated uncertainties (±) in these values are given in parentheses. The peak widths also have been corrected for the broadening effects of the Lorch window function used in Fourier transformation.

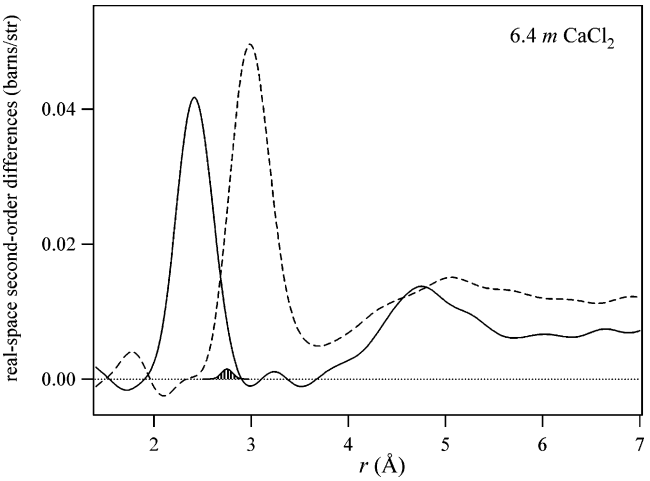

Figure 6. The second-order differences, $G_{Ca-X}(r)$ (solid curve) and $G_{Ca-H}(r)$ (dashed curve), for the high concentration, illustrating the effectiveness of this method for separating the peaks in the first hydration shell. The exceptional quality of the results is borne out by the close match (to within 2%) in the water coordination numbers estimated from the first hydration peaks. This small difference in coordination numbers can be used to estimate an upper detection limit for Ca−Cl contact ion pairing by modeling, using a Gaussian peak centered at $r = 2.75$ Å (hatched curve). The result is a coordination number of less than 0.1, confirming the absence of significant ion pairing even at this high concentration.

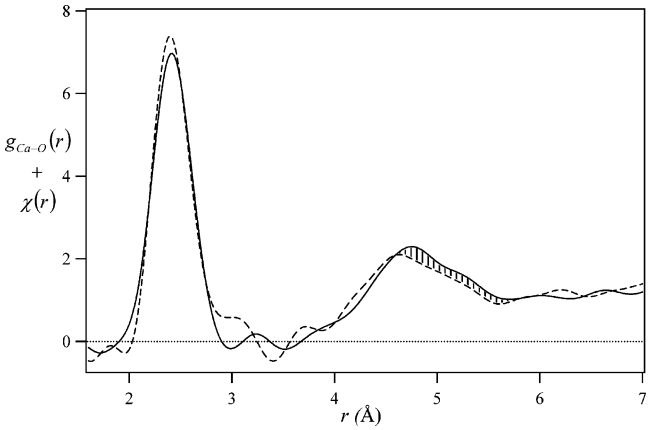

Figure 7. The changes in the Ca−X pair distribution function going from low (dashed curve) to high (solid curve) concentration. What is actually plotted for the higher concentration is a reduced pair distribution function, $0.92[g_{Ca-O}(r) + \chi(r)]$, so that relative changes in coordination number are more apparent. The broad increase in intensity in the region $4.6 < r < 5.6$ Å (hatched region) appears to be due to Cl^- ions entering the second hydration shell at the higher concentration.

coordination numbers estimated independently from each first peak in the second-order differences (see Table 5). This also suggests the net effect of the error terms is negligible even in the low-*r*, first hydration shell region. The small difference in coordination numbers can hence be used to estimate an upper (detection) limit for the amount of contact ion pairing by modeling the possible Ca−Cl contribution to the Ca−X function as a Gaussian peak with appropriate parameters for the width and position (fwhm = 0.1 Å, $r_{peak} = 2.75$ Å).[21] Adjusting the peak amplitude to eliminate the small discrepancy in hydration numbers (see Figure 6) suggests an average coordination number of less than 0.1 Cl^- ions around each Ca^{2+}, confirming the absence of significant contact ion pairing even at this high concentration. Due to the exceptional conditioning of the present neutron data, our estimated upper limit for Ca−Cl contact ion pairing is comparable to that provided by EXAFS—ostensibly, a much more sensitive technique—in our earlier study shown in part I.

Comparing the second-order differences in detail allows a compelling picture of the effects of concentration on the Ca^{2+} solvation structure to emerge. Figure 7 illustrates the changes in the Ca−X pair distribution function. What is actually plotted for the higher concentration is a reduced function, $0.92[g_{Ca-O}(r) + \chi(r)]$, taking into account the lower number density and oxygen atom concentration (see Table 2), so that areas under peaks better reflect changes in coordination number. Consistent with our earlier comparison of first-order differences, there is no significant change in the Ca−O first peak aside from a small reduction in size and hence coordination number (Table 5). The Ca−O first peak also remains well separated from the second hydration shell by a deep minimum that goes essentially to zero, suggesting no substantive change in the dynamics of water molecule exchange between the first and second hydration shells. The most substantial difference at high *r* is a marked increase in the region $4.6 < r < 5.6$ Å. This range of distances is consistent with Ca−Cl contributions due to Cl^- ions entering the second hydration shell around Ca^{2+} and forming solvent-shared ion pairs. Assuming the increase is entirely due to Ca−Cl (eq 12), approximately 1.8 ± 0.2 Cl^- ions enter the second hydration shell as the concentration is increased. This compares to a coordination number of about 5 Cl^- ions estimated from XANES spectra in part I. Note that the present result should be regarded as a lower limit since we have only estimated the *increase* over that at lower concentration. We have also implicitly assumed no change in $g_{Ca-O}(r)$ for the second hydration shell region—even though there is some evidence of this from the small decrease in intensity in the range $4 < r < 4.5$ Å.

The changes in the Ca−H pair distribution function with concentration (Figure 8) are also strongly consistent with the entry of counterions into the second hydration shell. Again, what has been plotted for the high concentration is actually a reduced function, $0.92g_{Ca-H}(r)$, taking into account the lower number density and hydrogen atom concentration. The notable broadening of the second hydration shell is consistent with Cl^- ions changing the orientation of water molecules via their positively charged hydrogen atoms. This picture naturally suggests a lesser impact on the Ca−O pair distribution, which does indeed appear to be the case and is consistent with our interpretation of the changes in the measured Ca−X function. The possibility that the increased disorder in the Ca−H distribution is dynamic in

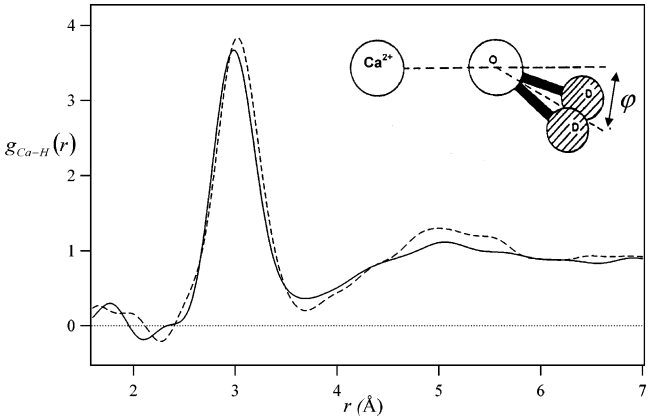

Figure 8. The changes in the Ca−H pair distribution function going from low (dashed curve) to high (solid curve) concentration. Again, what is actually plotted for 6.4 *m* $CaCl_2$ is a reduced pair distribution function, $0.92g_{Ca-H}(r)$, which takes into account the lower number density and atom fraction of hydrogen at the higher concentration. The inset figure illustrates how a water molecule can tilt on the surface of the Ca^{2+} ion and the definition of the tilt angle, φ. Assuming there is always close contact between the cation and water oxygen, any symmetrical tilt away from the dipole ($\varphi = 0$) orientation results in shorter ion−hydrogen distances.

origin and due to greatly increased exchange of water molecules in and out of the first hydration shell (as perhaps suggested by the filling-in of the first minimum at $r \approx 3.7$ Å) can be ruled out because of the lack of change in the Ca−X first minimum. Despite the broadness of the second peak in $g_{Ca-H}(r)$, it is possible to estimate the average number of water molecules in the second hydration shell. Using consistent radial limits ($r1 = 3.7$ and $r2 = 6.0$ Å) for the integration of peak areas (eq 10), we obtain values of 20.3 and 18.7, respectively, going from low to high concentration. Although the absolute coordination number values vary depending on the precise choice of $r1$ and $r2$, the difference with concentration is consistently about 1.6 water molecules. Given that a water molecule occupies nearly the same volume (30 $Å^3$) as a Cl^- ion (25 $Å^3$), it seems reasonable that the counterions displace a similar number of water molecules as they enter the second hydration shell. By disrupting hydrogen bonding between first- and second-shell waters, the Cl^- ions can also be expected to affect the orientation of water molecules in the first hydration shell. Such an effect is evident in Figure 8 where the Ca−H first peak clearly shifts to lower r at high concentration (just as indicated in the earlier comparison of first-order differences in Figure 5). It is now possible to understand this change in terms of a modified, probably more disordered and broadened, distribution of water tilt angles, $P(\cos\varphi)$, around the central Ca^{2+} ion. The inset in Figure 8 shows how a water molecule can tilt on the Ca^{2+} ion surface and the definition of the tilt angle, φ. Although it is not possible to obtain direct information about $P(\cos\varphi)$ from diffraction data,[22] modeling studies by Powell and Neilson[23] show that for a distribution centered around the dipole orientation, $\varphi = 0$, broadening generally causes the calculated ion-H peak to shift to lower r. It is, of course, also possible that there is a shift in the *center* of the distribution without significant broadening, i.e., an increase in the mean tilt angle and hence a reduction in the average ion−H distance. In either case, the effect on the Ca−H first peak can be ascribed to the presence of Cl^- ions in the second hydration shell.

It is further illuminating to compare the present findings to those of Hewish et al.[9] also using neutron scattering and calcium isotope substitution. This earlier study is limited to first-order differences because only solutions in heavy water (1.0, 2.8, and 4.5 *m* $CaCl_2$) were measured. Our Ca−O and Ca−H first peak distances for the 4.0 *m* concentration (Table 5) agree closely with values of 2.41 and 3.04 ± 0.03 Å, respectively, reported by Hewish et al. for their 4.5 *m* solution. However, their reported coordination number of 6.4 ± 0.3 at the same concentration appears to be on the low side compared with the present results which indicate closer to 7 water molecules in the first hydration shell around Ca^{2+}. Given the greater rigor and consistency required for a successful second-order difference experiment, we believe the present results for coordination number are more reliable. The most striking observation made by Hewish et al was a strong composition dependence of the water coordination number which they report as declining from as much as 10 at 1.0 *m* to less than 7 at 4.5 *m* concentration. Although the effect is not as pronounced, there is some evidence for this in the present results with the average coordination number declining by about 5% going from 4.0 to 6.4 *m* concentration. This change is broadly in line with the decrease in overall atomic number density between the two concentrations. If this trend is assumed to hold to low concentration then the limiting value of water coordination number is about 8—somewhat lower than the notably high value of 10 reported by Hewish et al. Of the crystalline solids, the $CaCl_2$ hexahydrate serves as the closest reference and has the highest coordination number with 9 waters surrounding each Ca^{2+} ion. Because the local environment in the disordered liquid state is often similar to that of the related solid—albeit with reduced symmetry and vacancies—this comparison also suggests a maximum hydration number in aqueous solution of close to 8. Our suggested maximum coordination number and the observed steady decline with concentration are both supported by the results of Katz et al.,[24] who used ab initio molecular orbital calculations to show that hydrated calcium clusters containing 6, 7, and 8 waters in the first hydration shell are energetically very similar, whereas all other coordination numbers have significantly higher energies. To directly verify our claims, new NDIS studies of $CaCl_2$ aqueous solutions at low concentration will be needed.

Summary and Final Remarks

The use of neutron diffraction with calcium isotope substitution in both light and heavy water has provided a unique window into the effects of concentration on the Ca^{2+} solvation structure in ambient aqueous solution. The results confirm many of the findings of the preceding EXAFS study, part I: specifically, minimal change in the nearest-neighbor Ca−O correlation, a mean coordination number of about 7 waters in the first hydration shell, and the absence of significant Ca^{2+}−Cl^- contact ion pairing even at concentrations as high as 6.4 *m* $CaCl_2$. The exceptional conditioning of the second-order isotope difference data even allows us to confirm a detection limit for contact ion pairs of approximately 0.1 Cl^- ions around each Ca^{2+} at the high concentration. By providing quantitative and unambiguous information on longer range structure, the present study directly confirms the suggestion in part I that the formation of Ca^{2+}−OH_2−Cl^- solvent-shared ion pairs—and not ion association as originally suggested by Phutella and Pitzer[11]—is the microscopic basis for the observed thermodynamic anomaly in the $CaCl_2$ aqueous system over this concentration range. The strongest evidence comes from changes observed in the second hydration shell region of the Ca−X and Ca−H real-space pair distribution functions. Going from 4.0 to 6.4 *m* $CaCl_2$ concentration, there is a marked increase in the range $4.6 < r < 5.6$ Å of the Ca−X distribution, which we ascribe to Ca−Cl correlations. From this we estimate approximately 1.8 ± 0.2 Cl^- ions enter the second

hydration shell as the concentration is increased. Comparison of the unambiguous Ca−H pair distributions indicates the corresponding displacement of approximately 1.6 water molecules out of the second hydration shell. The presence of significant numbers of Cl^- ions in the second shell inevitably affects the orientation of water molecules in this layer, a fact borne out by the markedly broader and more disordered Ca−H distribution for distances greater than 3.7 Å. In addition to perturbing the radial alignment of second-shell water molecules via interactions with their hydrogen "legs", the presence of Cl^- ions also affects the orientation of water molecules in the *first* hydration shell. This is strikingly evident from the behavior of the Ca−H first peak, which shifts lower in position from $r =$ 3.03 to 2.98 Å as the concentration is raised, reflecting a modified (probably broader and more disordered) distribution of water molecule tilt angles.

As well as complementing and extending the preceding EXAFS investigation I, the present study also sheds intriguing light on the results of the earlier NDIS study by Hewish et al. covering a lower concentration range (1.0−4.5 *m* $CaCl_2$). Although our results confirm the concentration dependence of the first-shell hydration number, the effect appears to be less pronounced than previously reported. Of the two most comparable concentrations studied, our value of 7.25 ± 0.1 (using the unambiguous Ca−H function) for the average water coordination number at 4.0 *m* concentration also differs significantly from the value of 6.4 ± 0.3 reported by Hewish et al. for 4.5 *m* $CaCl_2$. Because of the greater precision and rigor required for second-order difference measurements, we are confident our results for coordination number are more reliable. However, the questions posed by the present study regarding the upper limit of coordination number in dilute solution and the degree of concentration dependence can only be fully addressed by renewed investigations of this system at lower concentrations.

To sum up, our findings strongly indicate the concentration range studied (4.0−6.4 *m*) is characterized by increasing numbers of ions with overlapping first hydration shells but only minimal ion pairing. It thus appears to represent a transition region between the well-separated and independently hydrated ions typical at lower concentration and an increasingly molten salt-like, hydrous structure evident at higher concentrations as exemplified by the hydrate melts.[25] The observed relaxation of the Ca^{2+} solvation structure to accommodate the competition from counterions for the dwindling number of hydration waters may also have wider implications. For one thing, it helps to explain the markedly higher saturation solubility of ambient $CaCl_2$ aqueous solutions (7.2 *m*, and as much as 9.25 *m* when supersaturated) compared to solutions of similar salts such as $MgCl_2$ (5.5 *m*).[26] Although the concentrations in living cells are 3 orders of magnitude lower than those in the present study, obvious questions also arise as to the behavior in biological systems when weakly hydrated Ca^{2+} ions drift close to protein and membrane surfaces covered with strongly bound water and experience what is effectively a *local* shortage of available water molecules. The subtle nature and adaptability of the Ca^{2+} hydration structure could conceivably play an important role in the process of dehydration that must precede binding to sites on proteins and entry into ion-conducting channels. Theoretical studies could provide deeper insights into such questions and in that context the detailed and unambiguous structural information provided by the present study will serve as an exacting test of the interatomic potentials or density functional approximations employed in simulation.

Acknowledgment. This research was sponsored by the Division of Chemical Sciences, Geosciences, and Biosciences, Office of Basic Energy Sciences, U.S. Department of Energy under contract DE-AC05-00OR22725 with Oak Ridge National Laboratory, managed and operated by UT-Battelle, LLC. The authors also acknowledge the sterling support from Pierre Palleau of the D4 instrument team. We also thank John L. Fulton (Pacific North-West National Lab.) and Brian Annis (ORNL) for fruitful discussions.

Supporting Information Available: Manual describing the correction program for neutron diffraction data. This material is available free of charge via the Internet at http://pubs.acs.org.

References and Notes

(1) Fraústo da Silva, J. J. R.; Williams, R. J. P. *The Biological Chemistry of the Elements*; Clarendon Press: Oxford, UK, 1991.

(2) See, e.g., Figure 1 and associated references in: Spångberg, D.; Hermansson, K.; Lindqvist-Reis, P.; Jalilehvand, F.; Sandström, M.; Persson, I. *J. Phys. Chem. B* **2000**, *104*, 10467−10472.

(3) Ohtaki, H.; Radnai, R. *Chem. Rev.* **1993**, *93*, 1157−1204.

(4) Guàrdia, E.; Sesé, G.; Padró, J. A.; Kalko, S. G. *J. Sol. Chem.* **1999**, *28*, 1113−1126.

(5) Obst, S.; Bradaczek, H. *J. Phys. Chem.* **1996**, *100*, 15677−15687.

(6) Probst, M. M.; Radnai, T.; Heinzinger, K.; Bopp, P.; Rode, B. M. *J. Phys. Chem.* **1985**, *89*, 753−759.

(7) Naor, M. M.; Nostrand, K. V.; Dellago, C. *Chem. Phys. Lett.* **2003**, *369*, 159−164.

(8) Bako, I.; Hutter J.; Palinkas, G. *J. Chem. Phys.* **2002**, *117*, 9838−9843.

(9) Hewish, N. A.; Neilson, G. W.; Enderby, J. E. *Nature* **1982**, *297*, 138−139.

(10) Fulton, J. L.; Badyal, Y. S.; Simonson, J. M.; Heald, S. M. *J. Phys. Chem. A* **2003**, *107*, 4688−4696.

(11) Phutela, R. C.; Pitzer, K. S. *J. Sol. Chem.* **1983**, *12*, 201−207.

(12) Jalilehvand, F.; Spångberg, D.; Lindqvist-Reis, P.; Hermansson, K.; Persson, I.; Sandström, M. *J. Am. Chem. Soc.* **2001**, *123*, 431−441.

(13) Powell, D. H.; Neilson, G. W.; Enderby, J. E. *J. Phys.*: *Condens. Matter* **1989**, *1*, 8721−8733.

(14) Broadbent, R. D.; Neilson, G. W.; Sandstrøm, M. *J. Phys.*: *Condens. Matter* **1992**, *4*, 639−648.

(15) Sears, V. F. *Neutron News* **1992**, *3* (3), 29−37.

(16) Badyal, Y. S.; Simonson, J. M.; Annis, B.; Londono, J. D. *J. Neutron Res.* **2002**, *10* (1), 19−29.

(17) Fischer, H. E.; Cuello, G. J.; Palleau, P.; Feltin, D.; Barnes, A. C.; Badyal, Y. S.; Simonson, J. M. *Appl. Phys. A*: *Mater. Sci. Process.* **2002**, *74*, S160−S162.

(18) Howe, M. A.; McGreevy, R. L.; Zetterström, P. *CORRECT*: A correction program for neutron diffraction data (version 2.23) 1998; http://www.studsvik.uu.se/Software/correct.htm.

(19) Neilson, G. W.; Enderby, J. E. *J. Phys. Chem.* **1996**, *100*, 1317−1322.

(20) Badyal, Y. S.; Simonson, J. M. *J. Chem. Phys.* **2003**, *119*, 4413−4418.

(21) This Ca−Cl contact ion pair distance is consistent with the crystal structure of the γ form of the tetrahydrate ($CaCl_2 \cdot 4H_2O$), which has the Ca atom surrounded by two Cl atoms and four water molecules, as determined by: Leclaire, P. A.; Borel, M. M.; Monier, J. C. *Acta Crystallogr.* **1980**, *B36*, 2757−2759.

(22) Szász, Gy. I.; Dietz, W.; Heinzinger K.; Pálinkas, G.; Radnai, T. *Chem. Phys. Lett.* **1982**, *92* (4), 388−392.

(23) Powell, D. H.; Neilson, G. W. *J. Phys.*: *Condens. Matter* **1990**, *2*, 3871−3878.

(24) Katz, A. K.; Glusker, J. P.; Beebe, S. A.; Bock, C. W. *J. Am. Chem. Soc.* **1996**, *118*, 5752−5763.

(25) Yamaguchi, T.; Hayashi, S.; Ohtaki, H. *Inorg. Chem.* **1989**, *28*, 2434−2439.

(26) *CODATA Thermodynamic Tables, Selections for Some Compounds of Calcium and Related Mixtures: A Prototype Set of Tables*; Gavin D., Parker, V. B., White, H. J., Jr., Eds.; Hemisphere Publishing Corp.: Washington, DC, 1987.